R E V I E W

Imaging of pediatric foot disorders

Alfonso Reginelli¹, Anna Russo¹, Fabrizio Turrizziani¹, Roberto Picascia¹,
Elisa Micheletti¹, Vittoria Galeazzi², Umberto Russo³, Assunta Sica¹, Fabrizio Cioce¹,
Alberto Aliprandi⁴,Andrea Giovagnoni⁵, Salvatore Cappabianca¹

¹ University of Campania "Luigi Vanvitelli", Department of Radiology, Naples, Italy; ² Azienda Ospedaliera Universitaria, Ospedali Riuniti di Ancona, Dipartimento di Scienze Radiologiche S. O. D. Radiologia Pediatrica e Specialistica, Ancona; ³ Department of Radiology, Parma Hospital, Parma, Italy; ⁴ Radiology Department of Physiotherapy and Rehabilitation, Istituti Clinici Zucchi, Monza (MB), Italy; ⁵ Azienda Ospedaliera Universitaria, Ospedali Riuniti di Ancona, Dipartimento di Scienze Radiologiche S. O. D. Radiologia Pediatrica e Specialistica, Università Politecnica delle Marche, Ancona

Summary. Infants and children undergo imaging studies to evaluate a wide variety of congenital and acquired disorders. Imaging protocols have to consider the patient's comfort, level of anxiety, and smaller size. The first imaging study is usually made with plain radiographs. The routine radiographic examination of the foot includes the anteroposterior (AP), lateral, and oblique projections. Magnetic Resonance Imaging (RMI) provides excellent anatomic detail of cartilage, vasculature and soft tissue thanks to superior soft tissue contrast and spatial resolution, so is valuable in many cases. According to the clinical and objective signs, guided by the radiographs images, we can be oriented to perform Computed Tomography (CT), CT imaging or MRI imaging. CT imaging is useful to observe the bones but it has the disadvantage of using radiation and doesn't adequately define the bone's non-ossified portions. On the contrary, MRI imaging is very useful in identifying the cartilaginous parts and vascular and soft tissues, thanks to its superior contrast and spatial resolution. Finally, it is important to orientate the diagnostic process keeping in mind the clinical sign of the patient and to use the most appropriate diagnostic technique. (www.actabiomedica.it)

Key words: pediatric foot, radiology, foot congenital disorders, foot acquired disorders

Introduction

Infants and children undergo imaging studies to evaluate a wide variety of congenital and acquired disorders. The first imaging study is conventional radiographs; sometimes they are performed with the need for additional imaging which is guided by the plain film findings and clinical presentation. Because children are usually less cooperative and their feet are smaller than adults, special care is needed when choosing and interpreting an imaging study. Imaging protocols have to consider the patient's comfort, level of anxiety, and smaller size. For instance, children younger than 7 years of age usually require sedation and continu-

ous monitoring during MR imaging; with regard to infants is needed positioning devices for conventional radiography. Furthermore, the bones become progressively more ossified as children grow-up and this must be considered when selecting and interpreting imaging studies. In this article, we review common injuries and unusual disorders of a child's foot and include a discussion on differential diagnosis: sesamoiditis, Kohler's disease, Freiberg infraction, Sever's disease, tarsal coalition, osteomyelitis, septic arthritis and tumors that might mimic a fracture. Knowledge of the anatomy and significance of accessory bones of the foot and disorders of the growing foot skeleton are helpful in managing injuries of child's foot (1-5).

Imaging

The first imaging study is usually made with plain radiographs. The routine radiographic examination of the foot includes the anteroposterior (AP), lateral, and oblique projections (6-10). In cases of suspected talocalcaneal coalition, it is often performed a Harris view of the calcaneus to evaluate the subtalar joint. Standing views provide the most reliable information about alignment and are required when evaluating children with clubfoot deformity. In infants, simulated standing techniques are necessary to assess the relationships between the ossification centers in the hindfoot and midfoot. This technique uses AP and lateral views and a solid plastic form to maintain the infant's foot in forced dorsiflexion to allow correct position of the foot (11-15). In children with suspected tarsal coalition, CT in the axial and coronal planes is performed. CT is also helpful in delineating the components of a fracture and in identifying the nidus in osteoid osteoma (16-18). Sonography has been used to visualize the non-ossified tarsal bones in infants with congenital foot anomalies. Magnetic Resonance imaging provides excellent anatomic detail of cartilage, vasculature and soft tissue thanks to superior soft tissue contrast and spatial resolution, so is valuable in many situations, including identifying the cartilaginous structures in the infant's foot during evaluation for clubfoot or skew foot, delineating articular cartilage, assessing the status of osteochondral fractures, and in the evaluation of avascular necrosis (19-25).

1. Congenital diseases

1.1 Congenital clubfoot

Congenital talipes equino-varus, or congenital clubfoot, is one of the most common abnormalities involving the foot.
Clubfoot has been classified into four types:
1. teratologic
2. positional
3. congenital
4. syndromic
The teratologic form is found in children with other underlying disorders, such as myelodysplasia and arthrogryposis.

Positional clubfoot deformity can result when a normal foot is maintained in an abnormal position in utero.

Congenital clubfoot is the most common form of this disorder and occurs in approximately 1:1000 live births. This deformity is usually isolated. It is more common in boys and may be bilateral in up to 50% of cases. The cause of congenital clubfoot is uncertain, but is thoughts it may be related to a deformity of the talus. Some studies have suggested a neuromuscular origin, they state that abnormal types and number of muscle fibers, changes in collagen synthesis, vascular hypoplasia, and some possible defects in anterior horn cells have been reported in infants and fetuses with clubfeet. Several anatomic components of the clubfoot deformity have been described. These include lateral rotation of the talus in the ankle joint, medial rotation of the calcaneus, talar and calcaneal equinus, medial subluxation of the navicular, medial subluxation of the cuboid, and multiple soft tissue contractures. Clinical evaluation of the infant clubfoot concerns in a variable degree of inflexibility; hindfoot varus and equinus; forefoot adduction; mild calf atrophy; and mild hypoplasia of the bones of the foot, tibia, and fibula.

There are some difficulties in positioning the foot for plain radiographs and MR imaging or the inability to visualize the cartilaginous anlage on CT, so the preoperative imaging assessment of the child with congenital clubfoot can be complicated. Radiographs have been the traditional method to evaluate the foot before repair. To perform AP and lateral projections, positioning devices have to be used to obtain forced dorsiflexion views of the foot. The position has to be as close to anatomic position as possible. This also applies to MR and CT imaging. On radiographs, the talocalcaneal angle is measured on both the AP and lateral projections. Normally this angle is between 20 and 40 degrees on the AP view and 35 and 50 degrees on the lateral view. In clubfoot with hindfoot equinovarus, the angle is reduced on both projections because of the abnormal relationship between the talus and the calcaneus (26-28).

In the infant foot, however, a large percentage of the foot is cartilaginous and CT does not adequately define the nonossified portions of the tarsals or the intertarsal joints.

MR imaging with its superior soft tissue contrast has proved to be valuable in preoperative evaluation. In fact, it can clearly demonstrate the ossified and cartilaginous portions of the tarsal bones and the intertarsal joints. However, the deformed clubfoot, is difficult to evaluate in standard orthogonal planes, so multiplanar reconstruction techniques should be used to classify the severity of clubfoot deformities. By the use of this multiplanar reconstruction software, images of even the most deformed foot can be rotated and adjusted until the tibiotalar joint, talocalcaneal joint; moreover talonavicular and calcaneocuboid relationships can be assessed in near anatomic planes (28-32). Wang et all. found that to have high-resolution images, data have to be acquired in three dimensional data sets. Slice misregistration was a problem for data acquired in two-dimensional sequences, otherwise, on three-dimensional T2-weighted images, cartilage could be clearly distinguished from adjacent soft tissue; the joint spaces were well-delineated on T1-weighted images and with inversion recovery pulses sequences were also beneficial in distinguishing cartilage from soft tissue and delineating the joint spaces. The drawback to complex multiplanar reconstruction evaluations is the time required for postprocessing, reported to be up to 35 minutes per case, depending on user familiarity with the program.

It is possible to identify clubfoot deformity with prenatal ultrasound and prenatal MR imaging. Both methods are valuable in detecting and assessing the severity of clubfoot deformity and identifying associated abnormality. Both imaging modalities may be used to assess fetuses with complicated diagnostic situations, when the maximal data are necessary for prenatal and perinatal management of a pregnancy.

Treatment of clubfoot usually begins with nonoperative management, including physical therapy, splints, and serial casting. If correction has not been achieved by 3 months of age, surgical treatment is indicated. The success rate for conservative management is low, approximately 5%. Surgical management includes a combination of soft tissue releases, tendon transfers, and osteotomies, (tendon transfers and bony procedures, that are most often used for recurrent deformities). Complete soft tissue release is the most common initial surgical procedure and includes release of posterior, medial, lateral, and anterior structures and incision of plantar soft tissues. Most repairs include the use of an internal fixation Kirschner wire, to maintain alignment across the talonavicular joint.

Most surgical treatments are performed when the patient is about 6 months of age. This is controversial, however, because some orthopedic surgeons believe that the ideal time for surgical treatment is when the child is between 3 to 6 months of age and others suppose that 9 to 12 months is better. Early surgery proponents consider that more opportunity exists for growth and remodeling during the first year, with resultant better correction and greater stability. Late surgery proponents argue in favor of the larger size of the foot and safer anesthesia. Satisfactory outcomes are achieved in 72% to 88% percent of surgical repairs.

Following initial repair of the clubfoot, the most common problem is a dynamic or fixed cavovarus deformity. Correction of the dynamic deformity is usually achieved with a tibialis anterior transfer. Fixed cavovarus deformity may require additional soft tissue releases and osteotomies. Complications of clubfoot surgery include wound dehiscence, infection, damage to the neurovascular bundle, and avascular necrosis of talus and less commonly the navicular. Rocker-bottom foot results when the equinus deformity is corrected without sufficient derotation of the calcaneus on the talus. This severe complication is difficult to resolve without surgical manipulation. As the child grows, calf atrophy, leg length discrepancy, and small foot size may become apparent, although the degree of asymmetry is usually not severe.

1.2 Metatarsus adductus and skewfoot

Adduction of the forefoot is one of the most common foot deformities found in children. Metatarsus adductus consists of adduction of the forefoot, with normal alignment in the midfoot and hindfoot. Most cases resolve spontaneously and require no treatment or radiographic evaluation. However, in severe cases, stretching or serial casting may be needed. Operative management may be needed in children older than 4 years of age or in cases resistant to more conservative treatment.

Skewfoot is considered to be a severe form of metatarsus adductus, includes valgus alignment in the hind-

foot, lateral subluxation of the navicular, and adduction of the metatarsals. Although some skewfoot correct spontaneously as the child grows, children with skewfoot require conservative or surgical management more often than those with metatarsus adductus. Skewfoot resembles metatarsus adductus on physical examination and it is difficult to distinguish between in the chubby infant foot. The radiographic evaluation is limited by the lack of ossification in the tarsals, while MR imaging has proved to be very valuable defining the tarsal positions in infants whose bones are not ossified. Hubbard et all. were able to delineate lateral displacement of the navicular relative to the talus and medial subluxation of the first metatarsal on the medial cuneiform. They compared these relationships with radiographs and found that when the base of the first metatarsal is lateral to the midtalar axis, the navicular is laterally subluxed on the talus. This finding helps to distinguish between metatarsus adductus and skewfoot. Treatment of resistant skewfoot includes serial casting, whilst symptomatic skewfeet usually require surgical correction.

1.3 Flatfoot and congenital vertical talus

Flatfoot is a descriptive term that includes several different causes that lead to valgus hindfoot and planovalgus foot. Flatfoot includes valgus rotation of the calcaneus on the talus with a resultant vertical alignment of the talus and flattening of the longitudinal arch of the foot. Flatfoot may be flexible or rigid. Flexible flatfoot or pronated foot is believed to be caused by ligamentous laxity permitting abnormal motion in the hindfoot. It is very common and usually asymptomatic. On radiographs, increased talocalcaneal angle is present on AP and lateral projections. Flatfoot may also be found in conditions with abnormal muscle tone, such as cerebral palsy, and rigid flatfoot with peroneal muscle spasm may be seen in tarsal coalition (33).

Congenital rigid flatfoot or congenital vertical talus is the most severe type of congenital flatfoot. It is characterized by dorsal dislocation of the navicular on the talus, vertical position of the talus, and plantar flexion of the calcaneus. Both the talus and the navicular have an abnormal profile: the navicular is wedge-shaped and the talar head is flattened. Half of patients with this deformity have other abnormalities, such as arthrogryposis, neurofibromatosis, myelomeningocele, and trisomies. On lateral radiographs it is possible to see the talus that lies almost parallel to the long axis of the tibia and the calcaneus, that is plantar flexed. These relationships remain fixed with plantar and dorsiflexion. MR imaging shows the relationships between the cartilaginous anlage of the tarsal bones before they are visible on radiographs. Treatment usually requires surgical management because conservative therapy with serial casting has not proven to be effective (34-41).

2. Osteochondral lesions

2.1 Osteochondritis dissecans of the talus

Osteochondritis dissecans of the talus is a transchondral fracture resulting from a torsional impaction of the tibia or the fibula on the articular surface of the talus; it may result in a medial or lateral talar fracture. Frequently, but not invariably, there is a history of a traumatic event involving inversion and dorsiflexion in case of a lateral defect or eversion and plantar flexion in the medial talar fracture. This lesion is most commonly found in boys in the second decade and most cases are unilateral.

Conventional radiography is the most common imaging modality used in the setting of ankle pain. In osteochondritis dissecans of the talus, a small focus of heterogeneous density or a small fracture line is seen in the medial or lateral aspect of the talar dome on the AP or mortise view of the ankle. A bone fragment may be visible. Traditionally, radiography has been used to grade osteochondritis dissecans of the talus; however, with the increase in diffusion of MR imaging, it is developed an MRI grading system.

In stage I, the articular cartilage over the lesion is thickened and the signal intensity in the cartilage is decreased. In stage II, there is disruption of the cartilage with decreased signal surrounding the fracture fragment. In stage III, increased signal intensity surrounds the fragment indicating extension of synovial fluid between the fragment and underlying bone. Stage IV shows a loose body. MR imaging provides information that helps to determine fragment viability and directs the treatment and it is also useful if postoperative follow-up is required.

The treatment for osteochondritis dissecans varies with the severity of the abnormality. Children and adolescents generally respond well to limitation of activity and immobilization. If there is separation of the fragment, however, early intervention is recommended and includes percutaneous drilling and arthroscopy or open surgery for removal of separated fragments.

Osteonecrosis of talar dome can mimic osteochondritis dissecans on MR imaging. However, the presence of a predisposing condition, such as talar neck fracture, corticosteroids, or vasculitis, and the presence of the characteristic double- rim sign on MR imaging with hyperintense inner rim and hypointense outer rim on T2-weighted images, makes differentiation easier.

Another differential diagnosis is possible in case of focal subchondral edema which is seen in both acute and chronic injury and following high-intensity exercise. They show up as ill-defined areas of high signal on T2-weighted sequences. These findings may persist for months after resolution of symptoms. In contrast to lesions with ill-defined reticular margin, well-defined subchondral lesions have about 50% chance of progressing to focal cartilage loss.

2.2 Other osteochondroses and osteonecroses

Common locations for osteochondroses and osteonecrosis in the foot include the tarsal navicular (Kohler disease) and the head of second or third metatarsal (Freiberg infraction).

- Kohler disease is an abnormality of endochondral ossification. Clinical presentation includes swelling, erythema, and tenderness along the medial foot. It is more commonly seen in boys between 3 and 10 years of age and may be bilateral in up to 25%. Diagnosis is based on clinical and radiographic findings, which shows sclerosis and fragmentation of the navicular ossification center, with preservation of surrounding cartilage.
- Freiberg infraction is traumatic osteonecrosis. The second metatarsal head is most commonly involved, followed by third metatarsal. It commonly affects adolescent girls, presenting with focal pain and tenderness. Plain radiographs are used for diagnoses, which show sclerosis and flattening of the metatarsal head, with increase in the metatarso- phalangeal joint space. MR imaging is used when radiographs show atypical images or when alternative etiologies, such as osteomyelitis or stress fracture, are considered. MR imaging shows low signal on both T1- and T2-weighted images, depending on the level of avascular sclerotic bone. It usually associates with joint effusion at the metatarsophalangeal joint, with edema in surrounding soft tissues.

3. Sever's disease (calcaneal apophysitis)

Sever's disease, also known as calcaneal apophysitis or calcaneoapophysitis, is a traction epiphysitis of the calcaneal apophysis, a cartilagineus growth center onto which inserts the Achilles tendon. It is more common in girls aged approximately 5 years and in boys aged 7 to 8 years. The growt center fuses in girls aged approximately 13 years and in boys aged 15 years. The most common etiologic theory of Sever's disease consider it as an overuse syndrome from repetitive microtrauma derived by increased traction on the apophysis. It's caused by running and jumping, which can induce avulsion fractures, followed by inflammation. The apophysis is thought to be more susceptible to injury for the rapid proliferation of cells in growth plates. Common in male child 10 to 12 years old, during growth spurt, they experience: pain over the apophyseal area of one or both heels and limited ankle joint dorsiflexion and biomechanical deformity; increased activity will worsen the pain and often, at the end of physical activity, the child will limp in order to take weight off the affected heel.

The radiographic imaging is not an adequate technique to diagnose this patology but the symptomatic fragmented apophysis usually is more dense than the asymptomatic apophysis; this testify inflammation. Radiographs are useful in differential diagnosis to exclude fractures and tumors (Fig. 1). Some authors described increased fragmentation of the calcaneal apophysis in the Sever's disease, which suggests greater mechanical stress during a vulnerable period, but not inflammation. In particular, MRI showed right calcaneal apophysis alterations, as: fragmentation(which was better

seen on T1 weighted-images), hyperintensity consistent with edema on fat saturated T2 weighted-images and enhancement following contrast administration on fat saturated T1 images. Other causes of musculoskeletal adolescent heel pain include achillobursitis, tenosynovitis, ankle sprains or peritendinitis, retrocalcaneal exostosis or bursitis, and plantar fasciitis.

4. Tarsal coalition

Tarsal coalition is a congenital bridging of two or more tarsal bones. The bridging may be fibrous (syndesmosis), cartilaginous (synchondrosis), or osseous (synostosis).

The incidence of tarsal coalition is classically thought to be approximately 1%; however, many Authors think that this is an underestimate as only the symptomatic cases come to attention (42). For example, cadaveric series has described an incidence of up to 13% (43-45).

Osseous coalition is generally evaluable on cross-sectional imaging (Fig. 2). Cartilaginous and fibrous coalitions may be more subtle on cross-sectional imaging, but generally are associated with some osseous deformity along the margin of the coalition (46). Tarsal coalitions are thought to be due to a failure of mesenchymal differentiation and segmentation, resulting in failure of normal tarsal joint formation (47-49). A possible autosomal dominant form of inheritance with variable penetrance has been proposed (50, 51). Most commonly, tarsal coalitions are observed in late childhood or adolescence. This is probably due to the fact that osseous coalitions usually ossify when patients are 8–16 years old, leading to restricted motion and subsequent symptomatology (42, 52, 53). In particular, calcaneonavicular coalitions occur in younger patients than talocalcaneal coalitions (8-12 years old versus 12-16 years old) due to the different normal ossification patterns of the tarsal bones (44, 54). The condition is bilateral in 25-50% of cases, although the two sides do not necessarily need to be symptomatic (55-58). Tarsal coalitions may clinically manifest as tarsal or hindfoot pain and stiffness, decreased subtalar motion, valgus deformity, and non-healing ankle sprains
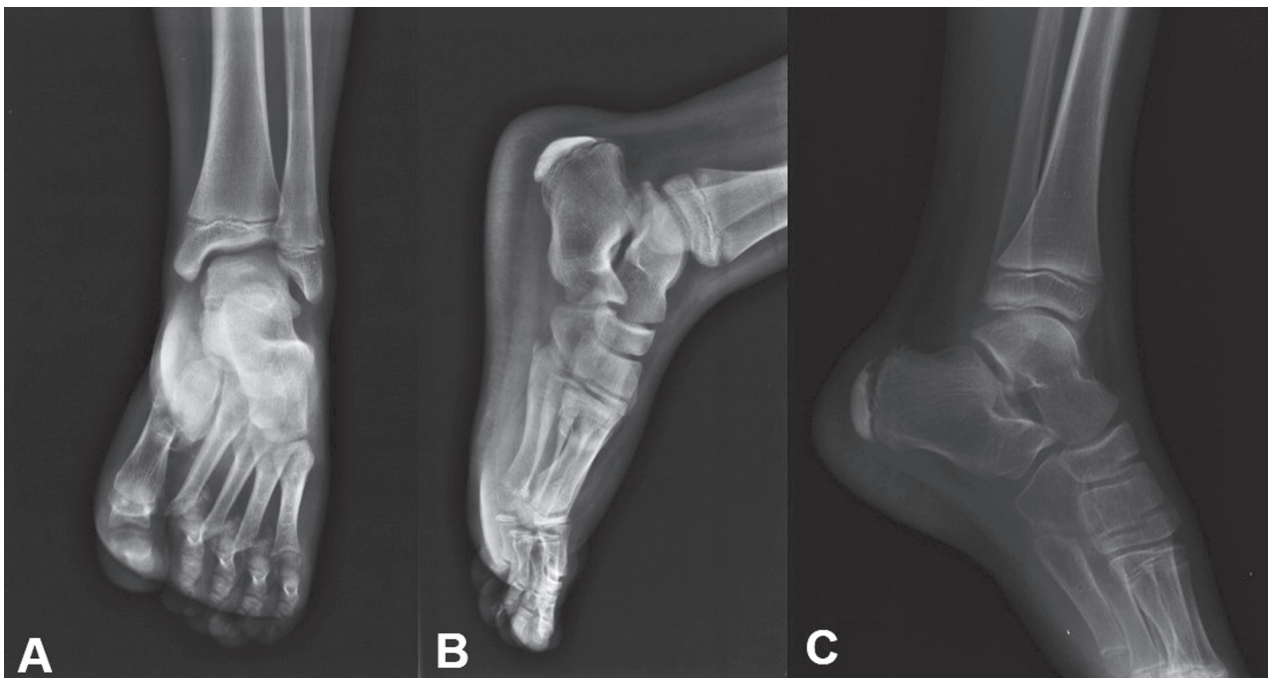

Figure 1. X-ray examination in different projections in a case of Sever-Blanke osteochondrosis in patient with calcaneodynia. It show sclerotic and slightly diastasis appearance of the calcaneal growth nucleus
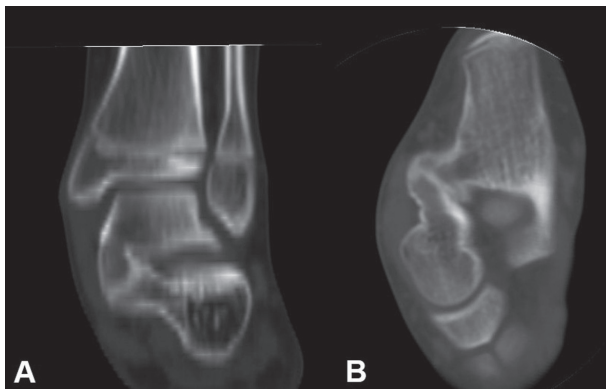
Figure 2. Multidetector computed tomography with MPR reconstruction in axial and coronal plane of medial calcaneal astragalus synostosis

(49, 59, 60). Symptoms of coalition include peroneal spastic flatfoot, rigid flatfoot attributed to peroneal spasm, or adaptive peroneal shortening in response to heel valgus (44, 61). Treatment options range from conservative to surgical. More conservative options include arch supports for minor symptoms, a short-leg walking cast for immobilization in neutral or a slight varus position with decreased activity, and/ or anti-inflammatory medications. Surgical treatments are typically reserved for recalcitrant cases, and surgical options include resection of an abnormal osseous bar with arthrodesis or primary arthrodesis (44). Radiographic imaging of tarsal coalition is generally the first imaging test performed, as it is readily available and relatively inexpensive. There are several direct and indirect findings that may be seen in the setting of tarsal coalition. CT and MR imaging characteristics are remarkably similar.

Radiographic findings in the setting of tarsal coalition may be divided into direct and indirect findings. Direct findings demonstrate an osseous continuity between two tarsal bones in the setting of osseous coalition. Indirect findings are more subtle. In the case of non-osseous coalitions, the two involved bones can demonstrate abnormal narrowing and irregularity of the involved joint space, which may radiographically appear to be degenerative changes. The patient's age may also a clue to the interpreter, as sometimes these degenerative changes will be present in a relatively young patient. Additionally, numerous signs indica-

tive of tarsal coalitions have been described, including the talar beak sign, C sign, drunken waiter sign, absent middle facet sign, and anteater sign.

Depending on the type of coalition that is present, different CT findings will be present. Osseous coalitions are mostly straightforward and will demonstrate abnormal osseous continuity of the two bones. Non-osseous coalitions are generally more subtle and manifest as abnormal narrowing of the joint space with minimal marginal reactive osseous changes. Sometimes, non-osseous coalitions have an imaging appearance similar to osteoarthritis, with joint space narrowing, eburnation, and subchondral cystic changes in one of the tarsal joints in an otherwise normal, non-arthritic appearing foot. As previously mentioned, the patient's age may also clue in the interpreter.

MR imaging demonstrates various abnormalities, depending on whether the coalition is osseous, cartilaginous, or fibrous. In osseous coalitions, bone marrow signal will continue across the fused articulation, seen as high signal intensity on T1-weighted images and low-signal intensity on T2-weighted fat-suppressed images, similar to normal bone marrow. Non-osseous coalitions demonstrate narrowing of the affected joint space, and irregularity of the bone interface is a common feature of cartilaginous and fibrous coalitions. Commonly, there may be bone marrow edema in the region of the coalition (62). In addition, cartilaginous coalitions will generally have signal intensity similar to fluid or cartilage, which will manifest as intermediate T1 signal and intermediate to-hyperintense T2 signal. On the contrary, fibrous coalitions will show low-signal intensity on all pulse sequences across the affected joint. While the findings of cartilaginous versus fibrous coalitions can at times be easy to define, many times the imaging characteristics are difficult to definitively categorize; in these cases, we prefer to state that there is a non-osseous tarsal coalition with findings that preclude definitive characterization.

5. Pediatric foot fractures

Foot fractures represent 5% to 8% of all pediatric fractures and approximately 7% of all physeal fractures. They usually have good prognosis and are treated non operatively with good results, but potential pitfalls in

the treatment of Lisfranc fractures, talar neck and body fractures. In these cases it must be anticipated or avoided if possible (10, 63-68).

Evaluation of fractures of the foot in children can be challenging, because the mechanism of injury sometimes in unknown; moreover bony injury may not be easily evident in largely cartilaginous tarsal bones, accessory bones and apophyses. (69-76)

5.1 Accessory bone and sesamoid

Accessory bone and sesamoids are normal findings but can be wrongly considered as fracture. Sesamoids and accessory ossicles usually have rounded smooth borders and are nontender, in contrast to fracture, which have sharp ragged edges and are tender. CT scans are useful to delineate the anatomy more clearly. MRI imaging shows the surrounding bone edema and aid in differentiating between fractures and sesamoid or accessory bones. The more frequent examples of accessory bones and sesamoid are:

- Os trigonum: accessory ossicle located close to the posterior process of the talus and may be mistaken for a fracture of the posterior process.
- Accessory navicular: accessory ossicle adjacent to the posteromedial navicular tuberosity.
- Hallux sesamoids: accessory ossicles located within medial and lateral slips of the flexor hallucis brevis. The medial or tibial sesamoid is larger and may be bipartited in up to four. They are subjected to pathological conditions including acute trauma, osteonecrosis and degeneration. Ossification at 8-10 years.
- Os peroneum: sesamoid bone in the peroneus longus tendon, near calcaneocuboid joint. Acute pain after fracture due to superfical peroneal nerve compression.
- Os intermetatarseum: as a free ossicle or as a spur between medial cuneiform and bases of the first and second metatarsal. When fractures are diagnosed, care should be taken to exclude Lisfanc injury (69).

5.2 Sesamoiditis

Repetitive injury to the plantar aspect of the forefoot can produce a sesamoiditis, which is a painful inflammatory condition. MR imaging findings in the marrow of the sesamoid bones include decreased or normal signal intensity on T1-weighted images and increased signal intensity on STIR images, similar to those caused by a stress response. If the signal intensity of the sesamoid bones is abnormal on STIR, but normal on T1-weighted images, sesamoiditis is a more probable diagnosis than a stress response. Involvement of both sesamoid bones also favors a diagnosis of sesamoiditis. Reactive soft-tissue abnormalities including tendinitis, synovitis, and bursitis are characteristic findings in sesamoiditis and are useful differentiating features (48).

5.3 Fractures of talus

The most common injury in children is a fracture of the neck of the talus, but also body, medial or lateral process and osteocondral injuries are possible. The major blood supply to the talus branches is guaranteed by the posterior tibial, dorsalis pedis and peroneal arteries. The interosseus tarsal canal contains the vascular anastomotic ring formed between the artery of the tarsal canal and the artery of the tarsal sinus (42, 77). Displaced fractures of the neck with disruption of this vascular ring have the potential for the development of avascular necrosis. Because the high cartilage-to-bone ratio in children, it is more resilient and resist bending forces than in adults (78). Most fractures of the talar neck result from forced dorsiflexion of the foot when the neck impinges against the anterior lip of the tibia; an associated fracture of the medial malleolus suggests a supination mechanism (44). Risk of avascular necrosis rise if the fracture is displaced and it can develop between a few weeks up to 6 months. Pain and swelling of the ankle and inability to bear weight are common symptoms. In undisplaced fractures, local signs may be absent (79-81).

Plain radiographs consisting of AP, lateral and oblique views and it should be done routinely. Canale and Kelly described a technique to obtain an improved view in AP projection: the foot is pronated to 15° and the x-ray tube is angled 75° to the tabletop (82). AP projection is helpful to find the "Hawkins's sign", subchondral lucency of the talar dome that occurs secondary to subchondral atrophy (43). This indicates that

there is sufficient vascularity in the talus, and is therefore pathognomonic for absence of avascular necrosis. It can occurs 6-8 weeks after a talar neck fracture and can be complete or incomplete (83). However, absence of Hawkins's sign does not necessarily indicate avascular necrosis in children and a MRI monitoring is needed. Magnetic resonance and bone scans may be useful during follow-up after treatment to monitor vascularity. Undisplaced fractures should be followed up for at least 18 months after injury. Displaced fractures and those with avascular necrosis need longer follow-up (51).

5.4 Fractures of metatarsal

They are the most common injuries in pediatric foot. They results from direct or indirect forces. Indirect or torsional forces usually produces fractures of the neck, and direct forces can fracture the shafts of the metatarsal. Children manifest swelling, pain and bruising of the forefoot. Fractures near the physis may affect the longitudinal growth and may lead to shortening and deficiency of the medial longitudinal arch. Avulsion fracture of the base of the fifth metatarsal is the most common isolated injury of the foot resulting from inversion or adduction force. Peroneus brevis commonly is responsible for this injury (84). The fracture line usually is perpendicular to the long axis of the shaft and displacement is minimal and may be confused with an apophyseal center or accessory ossicles (os vesalianum and os peroneum) (85). The apophyseal center appears around 8 years of age and fusion is complete by 12 years in girls and 15 years in boys. The long axis of the accessory center is parallel to the long axis of the shafts and displacement is minimal (Fig. 3) (69).

5.5 Jone's fracture

They are fractures that involve the proximal diaphysis of the of the fifth metatarsal (69).

5.6 Fractures of phalanges

They usually result from object falling on to the foot or stubbing a toe. These injuries heal rapidly within 3 or 4 weeks (69).
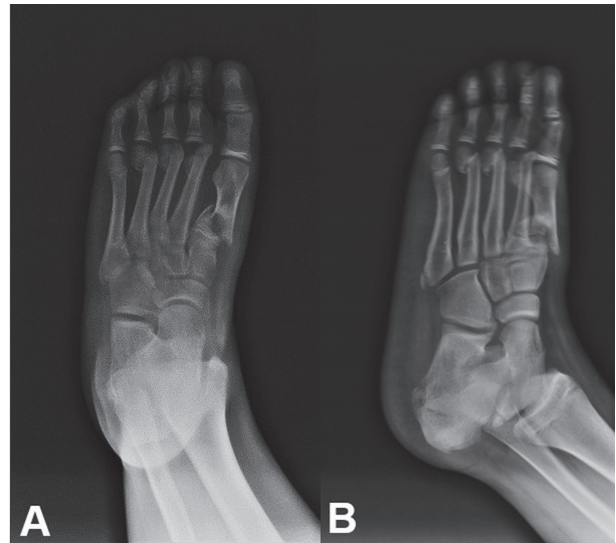

Figure 3. Traumatic lesions of midfoot with displaced fracture at the base of the I metatarsus (A), and of metatarsal heads of II, III, IV bone (B). X-ray examination is partly limited by poor patient collaboration

5.7 Tarsometatarsal injuries(Lisfranc injuries)

The bases of the three medial metatarsals articulate with the three cuneiforms medially and the cuboid supports the two lateral metatarsal. The base of the second metatarsal is recessed proximally in relation to the other tarsometatarsal joints and is well connected through ligaments to all cuneiforms. This joint is critical to the integrity of tarsometatarsal joint complex. Ligaments on the plantar side are stronger than thin dorsal ligaments, that poorly resist tensile forces. Injuries can result from direct forces (object falling onto the foot result in rupture of the strong plantar ligaments and metatarsal displaced in plantar direction with associated severe soft tissue injury) or indirect (violent plantar flexion or abduction force alone or in combination) (59).

Hardcastle classification(45)
- Type A: incongruity of entire tarsometatarsal complex in one plane, sagittal, coronal, or combined
- Type B: partial incongruity that may be medial displacement of the first metatarsal or lateral displacement of the four lateral metatarsal.
- Type C: the first metatarsal displaces medially

and any combination of lateral four metatarsal displace laterally.

Symptoms are pain and tenderness in midfoot region, inability to bear weight and dorsal or plantar ecchymosis (69).

6. Osteomyelitis

Osteomyelitis of the foot most often results from transcutaneous spread of soft tissue infection that involve bone at a later time. MR imaging findings in osteomyelitis include low signal intensity within the infected bone marrow on T1-weighted images, increased signal intensity on T2-weighted and STIR images, and contrast enhancement following intravenous administration of gadopentetate dimeglumine. Secondary signs include a cutaneous ulcer, cellulitis, phlegmon, soft-tissue abscess sinus tract, and cortical interruption (48).

7. Septic arthritis

Septic arthritis is often caused by the spread of infection from an adjacent soft-tissue or bone source. MR imaging findings include increased joint fluid and synovial thickening and enhancement. Marrow signal intensity changes and enhancement in the subarticular bone are similar to those seen in osteomyelitis. These findings are nonspecific and may also be seen in acute neuropathic disease and inflammatory arthritis. Soft-tissue signs of infection support the diagnosis of septic arthritis (48).

8. Hematopoietic marrow vs bone marrow edema on MRI imaging

On pediatric feet MRI images, high-signal T2-weighted bone marrow can be a normal finding, often seen in bone marrow edema, such as transient osteoporosis, trauma, inflammation, infection, vascular diseases, avascular necrosis, primitive and secundary tumors, arthritis, metabolic, iatrogenic, biomechanical factors and abnormal development, but also in hematopoietic marrow. Hematopoietic marrow shows symmetrical distribution (though asymmetries are available) and is more prominently represented as distal, for its specific proximal-to-distal migration pattern (from metatarsal bases to talus and heel) until it is no longer identifiable during puberty (no longer seen in 16 years old children). The changes were most commonly located in the calcaneus (54%), followed by the talus (35%) and navicular bone (35%), rarely plantar fascia insertion on heel or fibula. Hematopietic marrow on MRI imaging is high signal T2-weighted and STIR sequences and intermediate-low on T1 weighted. While the children grow, it becomes brighter than muscle until becomes similar to fat with low signal on T2-fat suppressed sequences. So, high-sensitive fluid sequences are required to highlight residual hematoipoietic marrow, that on T1-weighted could be misunderstood (86).

Conclusion

In conclusion, to evaluate congenital and acquired disorders in infant and children we can principally use plain radiographs, CT and MRI. The first imaging study is usually plain radiographs. After that, according to the clinical and objective signs, guided by the radiographs images, we can be oriented to perform CT imaging or MRI imaging. CT imaging is useful to observe the bones but it has the disadvantage of using radiation and doesn't adequately define the bone's nonossified portions. On the contrary, MRI imaging is very useful in identifying the cartilagineous parts and vascular and soft tissues, thanks to its superior contrast and spatial resolution. The disadvantage is due to the long-term acquisition of the sequences and the collaboration of the patients. Finally, it is important to orientate the diagnostic process keeping in mind the clinical sign of the patient and to use the most appropriate diagnostic technique.

Reference

1. Reginelli A, Zappia M, Barile A, Brunese L. Strategies of imaging after orthopedic surgery. Musculoskeletal Surg 2017; 101:
2. Di Pietto F, Chianca V, de Ritis R, Cesarano E, Reginelli A, Barile A, Zappia M, Ginolfi L. Postoperative imaging in arthroscopic hip surgery. Musculoskeletal Surg 2017; 101: 43-49.
3. Barile A, Bruno F, Mariani S, Arrigoni F, Brunese L, Zappia

M, Splendiani A, Di Cesare E, Masciocchi C. Follow-up of surgical and minimally invasive treatment of Achilles tendon pathology: a brief diagnostic imaging review. Musculoskeletal Surg 2017; 101: 51-61.

4. de Filippo M, Azzali E, Pesce A, Saba L, Mostardi M, Borgia D, Barile A, Capasso R, de Palmi F, Caravaggio F. CT arthrography for evaluation of autologous chondrocyte and chondral-inductor scaffold implantation in the osteochondral lesions of the talus. Acta Biomedica 2016; 87: 51-56.

5. Barile A, La Marra A, Arrigoni F, Mariani S, Zugaro L, Splendiani A, Di Cesare E, Reginelli A, Zappia M, Brunese L, Duka E, Carrafiello G, Masciocchi C. Anaesthetics, steroids and platelet-rich plasma (PRP) in ultrasound-guided musculoskeletal procedures. Br J Radiol 2016; 89:

6. Splendiani A, Perri M, Marsecano C, Vellucci V, Michelini G, Barile A, Di Cesare E. Effects of serial macrocyclic-based contrast materials gadoterate meglumine and gadobutrol administrations on gadolinium-related dentate nuclei signal increases in unenhanced T1-weighted brain: a retrospective study in 158 multiple sclerosis (MS) patients. Radiol Med 2017;

7. Barile A, Arrigoni F, Bruno F, Guglielmi G, Zappia M, Reginelli A, Ruscitti P, Cipriani P, Giacomelli R, Brunese L, Masciocchi C. Computed Tomography and MR Imaging in Rheumatoid Arthritis. Radiol Clin North Am 2017;

8. Barile A, Bruno F, Arrigoni F, Splendiani A, Di Cesare E, Zappia M, Guglielmi G, Masciocchi C. Emergency and Trauma of the Ankle. Semin Musculoskelet Radiol 2017; 21: 282-289.

9. Barile A, Arrigoni F, Zugaro L, Zappia M, Cazzato RL, Garnon J, Ramamurthy N, Brunese L, Gangi A, Masciocchi C. Minimally invasive treatments of painful bone lesions: state of the art. Med Oncol 2017; 34:

10. Arrigoni F, Barile A, Zugaro L, Splendiani A, Di Cesare E, Caranci F, Ierardi AM, Floridi C, Angileri AS, Reginelli A, Brunese L, Masciocchi C. Intra-articular benign bone lesions treated with Magnetic Resonance-guided Focused Ultrasound (MRgFUS): imaging follow-up and clinical results. Med Oncol 2017; 34:

11. Mariani S, La Marra A, Arrigoni F, Necozione S, Splendiani A, Di Cesare E, Barile A, Masciocchi C. Dynamic measurement of patello-femoral joint alignment using weight-bearing magnetic resonance imaging (WB-MRI). Eur J Radiol 84: 2571-2578.

12. Barile A, Conti L, Lanni G, Calvisi V, Masciocchi C. Evaluation of medial meniscus tears and meniscal stability: Weight-bearing MRI vs arthroscopy. Eur J Radiol 2013; 82: 633-639.

13. Masciocchi C, Lanni G, Conti L, Conchiglia A, Fascetti E, Flamini S, Coletti G, Barile A. Soft-tissue inflammatory myofibroblastic tumors (IMTs) of the limbs: Potential and limits of diagnostic imaging. Skelet Radiol 2012; 41: 643-649.

14. Masciocchi C, Conti L, D'Orazio F, Conchiglia A, Lanni G, Barile A, Errors in musculoskeletal MRI, Errors in Radiology, Springer-Verlag Milan 2012, pp. 209-217.

15. Barile A, Regis G, Masi R, Maggiori M, Gallo A, Faletti C, Masciocchi C. Musculoskeletal tumours: Preliminary experience with perfusion MRI. Radiol Med 2007; 112: 550-561.

16. Klauser A, Demharter J, De Marchi A, Sureda D, Barile A, Masciocchi C, Faletti C, Schirmer M, Kleffel T, Bohndorf K, group Is. Contrast enhanced gray-scale sonography in assessment of joint vascularity in rheumatoid arthritis: results from the IACUS study group. Eur Radiol 2005; 15: 2404-10.

17. Masciocchi C, Barile A, Lelli S, Calvisi V. Magnetic resonance imaging (MRI) and arthro-MRI in the evaluation of the chondral pathology of the knee joint. Radiol Med 2004; 108: 149-58.

18. Barile A, Sabatini M, Iannessi F, Di Cesare E, Splendiani A, Calvisi V, Masciocchi C. Pigmented villonodular synovitis (PVNS) of the knee joint: magnetic resonance imaging (MRI) using standard and dynamic paramagnetic contrast media. Report of 52 cases surgically and histologically controlled. Radiol Med 2004; 107: 356-66.

19. Lanzillo R, Prinster A, Scarano V, Liuzzi R, Coppola G, Florio C, Salvatore E, Schiavone V, Brunetti A, Muto M, Orefice G, Alfano B, Bonavita V, Brescia Morra V. Neuropsychological assessment, quantitative MRI and ApoE gene polymorphisms in a series of MS patients treated with IFN beta-1b Journal of the Neurological Sciences 2006; 245 (1-2): 141-145.

20. Briganti F, Marseglia M, Leone G, Briganti G, Piccolo D, Napoli M. Caranci F. Endovascular treatment of a small aneurysm of the superior cerebellar artery with a flow-diverter device. Neuroradiol J 2013; 26 (3): 327-331.

21. Briganti F, Delehaye L, Leone G, Sicignano C, Buono G, Marseglia M, Caranci F, Tortora F, Maiuri F. Flow diverter device for the treatment of small middle cerebral artery aneurysms. J Neurointervent Surg 2016; 8: 287-294.

22. Muccio CF, Caranci F, D'Arco F, Cerase A, De Lipsis L, Esposito G, Tedeschi E, Andreula C. Magnetic resonance features of pyogenic brain abscesses and differential diagnosis using morphological and functional imaging studies: A pictorial essay. J Neuroradiol 2014; 41: 153-167.

23. Caranci F, Briganti F, La Porta M, Antinolfi G, Cesarano E, Fonio P, Brunese L, Coppolino F. Magnetic resonance imaging in brachial plexus injury. Musculoskeletal Surg 2013; 97: S181-S190.

24. Briganti F, Tedeschi E, Leone G, Marseglia M, Cicala D, Giamundo M, Napoli M, Caranci F. Endovascular treatment of vertebro-vertebral arteriovenous fistula. A report of three cases and literature review. Neuroradiol J 2013; 26: 339-46.

25. Cappabianca S, Colella G, Russo A, Pezzullo M, Reginelli A, Iaselli F, Rotondo A. Maxillofacial fibrous dysplasia: personal experience with gadoliniumenhanced magnetic resonance imaging. Radiol Med 2008; 113: 1198-210.

26. Cappabianca S, Iaselli F, Negro A, Basile A, Reginelli A, Grassi R, Rotondo A. Magnetic resonance imaging in the evaluation of anatomical risk factors for pediatric obstruc-

tive sleep apnoea-hypopnoea: a pilot study. Int J Pediatr Otorhinolaryngol 2013; 77: 69-75.

27. Mandato Y, Reginelli A, Galasso R, Iacobellis F, Berritto D, Cappabianca S. Errors in the radiological evaluation of the alimentary tract: part I. Semin Ultrasound CT MR 2012; 33: 300-7.

28. Reginelli A, Silvestro G, Fontanella G, Sangiovanni A, Conte M, Nuzzo I, Di Lecce A, Martino A, Grassi R, Murino P, Cappabianca S. Performance status versus anatomical recovery in metastatic disease: The role of palliative radiation treatment. Int J Surg 2016; 33 Suppl 1: S126-31.

29. Reginelli A, Silvestro G, Fontanella G, Sangiovanni A, Conte M, Nuzzo I, Calvanese M, Traettino M, Ferraioli P, Grassi R, Manzo R, Cappabianca S. Validation of DWI in assessment of radiotreated bone metastases in elderly patients. Int J Surg 2016; 33 Suppl 1: S148-53.

30. Cappabianca S, Scuotto A, Iaselli F, Pignatelli di Spinazzola N, Urraro F, Sarti G, Montemarano M, Grassi R, Rotondo A. Computed tomography and magnetic resonance angiography in the evaluation of aberrant origin of the external carotid artery branches. Surg Radiol Anat 2012; 34: 393-9.

31. Scialpi M, Cappabianca S, Rotondo A, Scalera GB, Barberini F, Cagini L, Donato S, Brunese L, Piscioli I, Lupattelli L. Pulmonary congenital cystic disease in adults. Spiral computed tomography findings with pathologic correlation and management. Radiol Med 2010; 115 (4): 539-550.

32. Grassi R, Lombardi G, Reginelli A, Capasso F, Romano F, Floriani I, Colacurci N. Coccygeal movement: assessment with dynamic MRI. Eur J Radiol 2007; 61: 473-9.

33. Nurzynska D, DiMeglio F, Castaldo C, Latino F, Romano V, Miraglia R, Guerra G, Brunese L, Montagnani S. Flatfoot in children: Anatomy of decision making. Ital J Anat Embryol 2012; 117: 98-106.

34. Zappia M, Cuomo G, Martino MT, Reginelli A, Brunese L. The effect of foot position on Power Doppler Ultrasound grading of Achilles enthesitis. Rheumatol Int 2016; 36: 871-874.

35. Cuomo G, Zappia M, Iudici M, Abignano G, Rotondo A, Valentini G. The origin of tendon friction rubs in patients with systemic sclerosis: a sonographic explanation. Arthritis Rheum 2012; 64: 1291-3.

36. Aliprandi A, Di Pietto F, Minafra P, Zappia M, Pozza S, Sconfienza LM. Femoro-acetabular impingement: what the general radiologist should know. Radiol Med 2014; 119: 103-12.

37. De Filippo M, Pesce A, Barile A, Borgia D, Zappia M, Romano A, Pogliacomi F, Verdano M, Pellegrini A, Johnson K. Imaging of postoperative shoulder instability. Musculoskelet Surg 2017; 101: 15-22.

38. Cappabianca S, Colella G, Pezzullo MG, Russo A, Iaselli F, Brunese L, Rotondo A. Lipomatous lesions of the head and neck region: Imaging findings in comparison with histological type. Radiol Med 2008; 113: 758-770.

39. Pinto A, Brunese L, Pinto F, Acampora C, Romano L. E-learning and education in radiology. Eur J Radiol 2011; 78: 368-371.

40. Pinto A, Brunese L, Pinto F, Reali R, Daniele S, Romano L. The Concept of Error and Malpractice in Radiology. Semin Ultrasound CT MRI 2012; 33: 275-279.

41. Pierot L, Söderman M, Bendszus M, White P, Muto M, Turjman F, Mangiafico S, Gralla J, Fiehler J, Szikora I, Cognard C. Statement of ESMINT and ESNR regarding recent trials evaluating the endovascular treatment at the acute stage of ischemic stroke. Neuroradiology 2013; 55 (11): 1313-1318.

42. Mulfinger GL, Trueta J. The blood supply of the talus. J Bone Joint Surg Br 1970; 52: 160-7.

43. Hawkins LG. Fractures of the neck of the talus. J Bone Joint Surg Am 1970; 52: 991-1002.

44. Jensen I, Wester JU, Rasmussen F, Lindequist S, Schantz K. Prognosis of fracture of the talus in children. 21 (7-34)-year follow-up of 14 cases. Acta Orthop Scand 1994; 65: 398-400.

45. Hardcastle PH, Reschauer R, Kutscha-Lissberg E, Schoffmann W. Injuries to the tarsometatarsal joint. Incidence, classification and treatment. J Bone Joint Surg Br 1982; 64: 349-56.

46. Nicastro JF, Haupt HA. Probable stress fracture of the cuboid in an infant. A case report. J Bone Joint Surg Am 1984; 66: 1106-8.

47. Lawrence DA, Rolen MF, Haims AH, Zayour Z, Moukaddam HA. Tarsal Coalitions: Radiographic, CT, and MR Imaging Findings. HSS Journal 2014; 10: 153-166.

48. Ashman CJ, Klecker RJ, Yu JS. Forefoot Pain Involving the Metatarsal Region: Differential Diagnosis with MR Imaging. RadioGraphics 2001; 21: 1425-1440.

49. Dogan MS, Doganay S, Koc G, Gorkem SB, Ciraci S, Coskun A. Calcaneal Apophysitis (Sever's Disease): MRI Findings 2016 2016; 35: 3.

50. Scharfbillig RW, Jones S, Scutter SD. Sever's disease: what does the literature really tell us? J Am Podiatr Med Assoc 2008; 98: 212-23.

51. Kay RM, Tang CW. Pediatric foot fractures: evaluation and treatment. J Am Acad Orthop Surg 2001; 9: 308-19.

52. Russo A, Reginelli A, Zappia M, Rossi C, Fabozzi G, Cerrato M, Macarini L, Coppolino F. Ankle fracture: radiographic approach according to the Lauge-Hansen classification. Musculoskelet Surg 2013; 97 Suppl 2: S155-60.

53. Russo A, Zappia M, Reginelli A, Carfora M, D'Agosto GF, La Porta M, Genovese EA, Fonio P. Ankle impingement: a review of multimodality imaging approach. Musculoskelet Surg 2013; 97 Suppl 2: S161-8.

54. Zappia M, Castagna A, Barile A, Chianca V, Brunese L, Pouliart N. Imaging of the coracoglenoid ligament: a third ligament in the rotator interval of the shoulder. Skelet Radiol 2017; 46: 1101-1111.

55. Wester JU, Jensen IE, Rasmussen F, Lindequist S, Schantz K. Osteochondral lesions of the talar dome in children. A 24 (7-36) year follow-up of 13 cases. Acta Orthop Scand 1994; 65: 110-2.

56. Perrotta FM, Astorri D, Zappia M, Reginelli A, Brunese L, Lubrano E. An ultrasonographic study of enthesis in early psoriatic arthritis patients naive to traditional and biologic DMARDs treatment. Rheumatol Int 2016; 36: 1579-1583.

57. Zappia M, Carfora M, Romano AM, Reginelli A, Brunese L, Rotondo A, Castagna A. Sonography of chondral print on humeral head. Skelet Radiol 2016; 45: 35-40.

58. Zappia M, Di Pietto F, Aliprandi A, Pozza S, De Petro P, Muda A, Sconfienza LM. Multi-modal imaging of adhesive capsulitis of the shoulder. Insights Imaging 2016; 7: 365-71.

59. Wiley JJ. Tarso-Metatarsal Joint Injuries in Children. Journal of Pediatric Orthopaedics 1981; 1: 255-260.

60. Miele V, Di Giampietro I, Ianniello S, Pinto F, Trinci M. Diagnostic imaging in pediatric polytrauma management. Radiol Med 2014; 120: 33-49.

61. Cicala D, Briganti F, Casale L, Rossi C, Cagini L, Cesarano E, Brunese L, Giganti M. Atraumatic vertebral compression fractures: Differential diagnosis between benign osteoporotic and malignant fractures by MRI. Musculoskeletal Surg 2013; 97: S169-S179.

62. Schindler A, Mason DE, Allington NJ. Occult fracture of the calcaneus in toddlers. J Pediatr Orthop 1996; 16: 201-5.

63. Pinto A, Reginelli A, Pinto F, Lo Re G, Midiri F, Muzj C, Romano L, Brunese L. Errors in imaging patients in the emergency setting. Br J Radiol 2016; 89:

64. Masala S, Nano G, Marcia S, Muto M, Fucci FPM, Simonetti G. Osteoporotic vertebral compression fractures augmentation by injectable partly resorbable ceramic bone substitute (Cerament™|SPINE SUPPORT): A prospective nonrandomized study. Neuroradiology 2012; 54(11): 1245-1251.

65. Reginelli A, Russo A, Maresca D, Martiniello C, Cappabianca S, Brunese L. Imaging Assessment of Gunshot Wounds. Semin Ultrasound CT MRI 2015; 36: 57-66.

66. Cappabianca S, Porto A, Petrillo M, Greco B, Reginelli A, Ronza F, Setola F, Rossi G, Di Matteo A, Muto R, De Rimini ML, Piccolo S, Catalano M, Muto P, De Rosa N, Barra E, De Rosa I, Antinolfi F, Antinolfi G, Caputi M, Brunese L, Grassi R, Rotondo A. Preliminary study on the correlation between grading and histology of solitary pulmonary nodules and contrast enhancement and [18F] fluorodeoxyglucose standardised uptake value after evaluation by dynamic multiphase CT and PET/CT. J Clin Pathol 2011; 64 (2): 114-119.

67. Brunese L, Romeo A, Iorio S, Napolitano G, Fucili S, Zeppa P, Vallone G, Lombardi G, Bellastella A, Biondi B, Sodano A. Thyroid B-flow twinkling sign: a new feature of papillary cancer. Eur J Endocrinol 2008; 159 (4): 447-451.

68. Muto M, Perrotta V, Guarnieri G, Lavanga A, Vassallo P, Reginelli R, Rotondo A. Vertebroplasty and kyphoplasty: Friends or foes? Radiol Med 2008; 113: 1171-1184.

69. Ribbans WJ, Natarajan R, Alavala S. Pediatric foot fractures. Clin Orthop Relat Res 2005; 107-15.

70. Piccolo CL, Galluzzo M, Ianniello S, Trinci M, Russo A, Rossi E, Zeccolini M, Laporta A, Guglielmi G, Miele V. Pediatric musculoskeletal injuries: role of ultrasound and magnetic resonance imaging. Musculoskelet Surg 2017; 101: 85-102.

71. Piccolo CL, Ianniello S, Trinci M, Galluzzo M, Tonerini M, Zeccolini M, Guglielmi G, Miele V. Diagnostic Imaging in pediatric thoracic trauma. Radiol Med 2017;

72. Miele V, Piccolo CL, Trinci M, Galluzzo M, Ianniello S, Brunese L. Diagnostic imaging of blunt abdominal trauma in pediatric patients. Radiol Med 2016; 121: 409-430.

73. Miele V, Giampietro ID, Giannecchini S, Pizzi C, Trinci M, Pediatric polytrauma management, Imaging Trauma and Polytrauma in Pediatric Patients, Springer International Publishing 2015, pp. 1-28.

74. De Filippo M, Corsi A, Evaristi L, Bertoldi C, Sverzellati N, Averna R, Crotti P, Bini G, Tamburrini O, Zompatori M, Rossi C. Critical issues in radiology requests and reports. Radiol Med 2011; 116: 152-62.

75. Cataldi V, Laporta T, Sverzellati N, De Filippo M, Zompatori M. Detection of incidental vertebral fractures on routine lateral chest radiographs. Radiol Med 2008; 113: 968-77.

76. De Filippo M, Rovani C, Sudberry JJ, Rossi F, Pogliacomi F, Zompatori M. Magnetic resonance imaging comparison of intra-articular cavernous synovial hemangioma and cystic synovial hyperplasia of the knee. Acta Radiol 2006; 47: 581-4.

77. Aquino MD, Aquino L, Aquino JM. Talar neck fractures: a review of vascular supply and classification. J Foot Surg 1986; 25: 188-193.

78. Letts RM, Gibeault D. Fractures of the Neck of the Talus in Children. Foot & Ankle 1980; 1: 74-77.

79. De Filippo M, Pesce A, Barile A, Borgia D, Zappia M, Romano A, Pogliacomi F, Verdano M, Pellegrini A, Johnson K. Imaging of postoperative shoulder instability. Musculoskeletal Surg 2017; 101: 15-22.

80. Palma BD, Guasco D, Pedrazzoni M, Bolzoni M, Accardi F, Costa F, Sammarelli G, Craviotto L, De Filippo M, Ruffini L, Omede P, Ria R, Aversa F, Giuliani N. Osteolytic lesions, cytogenetic features and bone marrow levels of cytokines and chemokines in multiple myeloma patients: Role of chemokine (C-C motif) ligand 20. Leukemia 2016; 30: 409-16.

81. Barile A, Bruno F, Mariani S, Arrigoni F, Reginelli A, De Filippo M, Zappia M, Splendiani A, Di Cesare E, Masciocchi C. What can be seen after rotator cuff repair: a brief review of diagnostic imaging findings. Musculoskeletal Surg 2017; 101: 3-14.

82. Canale ST, Kelly FB, Jr. Fractures of the neck of the talus. Long-term evaluation of seventy-one cases. J Bone Joint Surg Am 1978; 60: 143-56.

83. Cannavò L, Ghargozloo D, Tomarchio A, Messina M, Massimino P. Inquadramento clinico, diagnostico e terapeutico delle AVN dell'astragalo Dipartimento di Specialità medico Chirurgiche - Sezione: Ortopedia e Traumatologia Università degli Studi di Catania 2010.

84. Richli WR, Rosenthal DI. Avulsion fracture of the fifth metatarsal: experimental study of pathomechanics. AJR Am J Roentgenol 1984; 143: 889-91.

85. Lawrence SJ, Botte MJ. Jones' fractures and related fractures of the proximal fifth metatarsal. Foot Ankle 1993; 14: 358-65.
86. Shabshin N, Schweitzer ME, Morrison WB, Carrino JA, Keller MS, Grissom LE. High-signal T2 changes of the bone marrow of the foot and ankle in children: red marrow or traumatic changes? Pediatr Radiol 2006; 36: 670-676.

Alfonso Reginelli, MD, PhD,
Department of Radiology, University of Campania
"Luigi Vanvitelli", Naples, Italy
E-mail: alfonsoreginelli@hotmail.com